

CONF-851007--14

STEADY STATE TEMPERATURE PROFILES IN TWO SIMULATED
LIQUID METAL REACTOR FUEL ASSEMBLIES
WITH IDENTICAL DESIGN SPECIFICATIONS*

A. E. Levin, J. J. Carbajo, D. B. Lloyd, B. H. Montgomery
S. D. Rose, J. L. Wantland

OAK RIDGE NATIONAL LABORATORY
Oak Ridge, Tennessee 37831

CONF-851007--14

DE86 002258

Submitted to the Third International Topical
Meeting on Nuclear Reactor Thermal-Hydraulics

October 15-18, 1985

Newport, Rhode Island

DISCLAIMER

This report was prepared as an account of work sponsored by an agency of the United States Government. Neither the United States Government nor any agency thereof, nor any of their employees, makes any warranty, express or implied, or assumes any legal liability or responsibility for the accuracy, completeness, or usefulness of any information, apparatus, product, or process disclosed, or represents that its use would not infringe privately owned rights. Reference herein to any specific commercial product, process, or service by trade name, trademark, manufacturer, or otherwise does not necessarily constitute or imply its endorsement, recommendation, or favoring by the United States Government or any agency thereof. The views and opinions of authors expressed herein do not necessarily state or reflect those of the United States Government or any agency thereof.

By acceptance of this article, the publisher and/or recipient acknowledges the U.S. Government's right to retain a nonexclusive, royalty-free license in and to any copyright covering this report.

*This research is sponsored by the Office of Breeder Reactor Projects, U.S. Department of Energy, under contract DE-AC05-84OR21400 with Martin Marietta Energy Systems, Inc.

MASTER

JSW

ABSTRACT

Temperature data from steady state tests in two parallel, simulated liquid metal reactor fuel assemblies with identical design specifications have been compared to determine the extent to which they agree. In general, good agreement was found in data at low flows and in bundle-center data at higher flows. Discrepancies in the data were noted near the bundle edges at higher flows. An analysis of bundle thermal boundary conditions showed that the possible eccentric placement of one bundle within the housing could account for these discrepancies.

Introduction

Temperature data from simulated reactor fuel assemblies are often used to develop and assess computer models for core thermal-hydraulic analysis. In a system with several bundles that have identical design specifications, such as a reactor core, small variations resulting from manufacturing and assembly tolerances can affect bundle thermal-hydraulic performance. In thermal-hydraulic calculations, these uncertainties are taken into account using statistically-derived hot channel factors. However, relatively few experimental data are available to make a quantitative assessment of these variations, particularly in liquid metal reactors (LMRs).

Using data from an out-of-pile liquid sodium loop containing two parallel simulated LMR fuel assemblies having identical design specifications, a comparison of steady state temperature data has been performed. These data were taken as part of the facility test program, and

included tests at high and low flows, with the power adjusted to provide a nominal power-to-flow ratio.

This paper includes a description of the test facility, the bundles and their instrumentation, and the tests used in this comparison. Data from these tests are presented and discussed, and reasons for differences in the data from the two bundles are explored.

Description of the Test Facility

The tests were performed in the Thermal-Hydraulic Out-of-Reactor Safety (THORS) facility at the Oak Ridge National Laboratory. The THORS facility is an engineering-scale, liquid sodium loop for the testing of simulated, electrically heated LMR bundles. The configuration of the loop for these tests, referred to as THORS-Shutdown Heat Removal System (SHRS) Assembly 1, is shown in Fig. 1. The two bundles are 19-pin assemblies of Large-Scale Prototype Breeder (LSPB) design specifications, connected to common upper and lower plena. A schematic of the bundle in its housing and in cross-section is shown in Fig. 2.

The facility is extensively instrumented with thermocouples, pressure transducers and flowmeters. The bundles also contain 118 thermocouples each, in both the fuel pin simulators (FPSs) and the wire-wrap spacers. All instrumentation is connected to the THORS computer-controlled data acquisition system (DAS), which can scan up to 500 channels at 10,000 points per second.

The loop can be configured to allow either forced convection or natural convection. In natural convection, flow passes up through the bundles into the upper plenum, then down through the intermediate heat exchanger (IHx) and the bypass line; the pump is used to supply only IHx

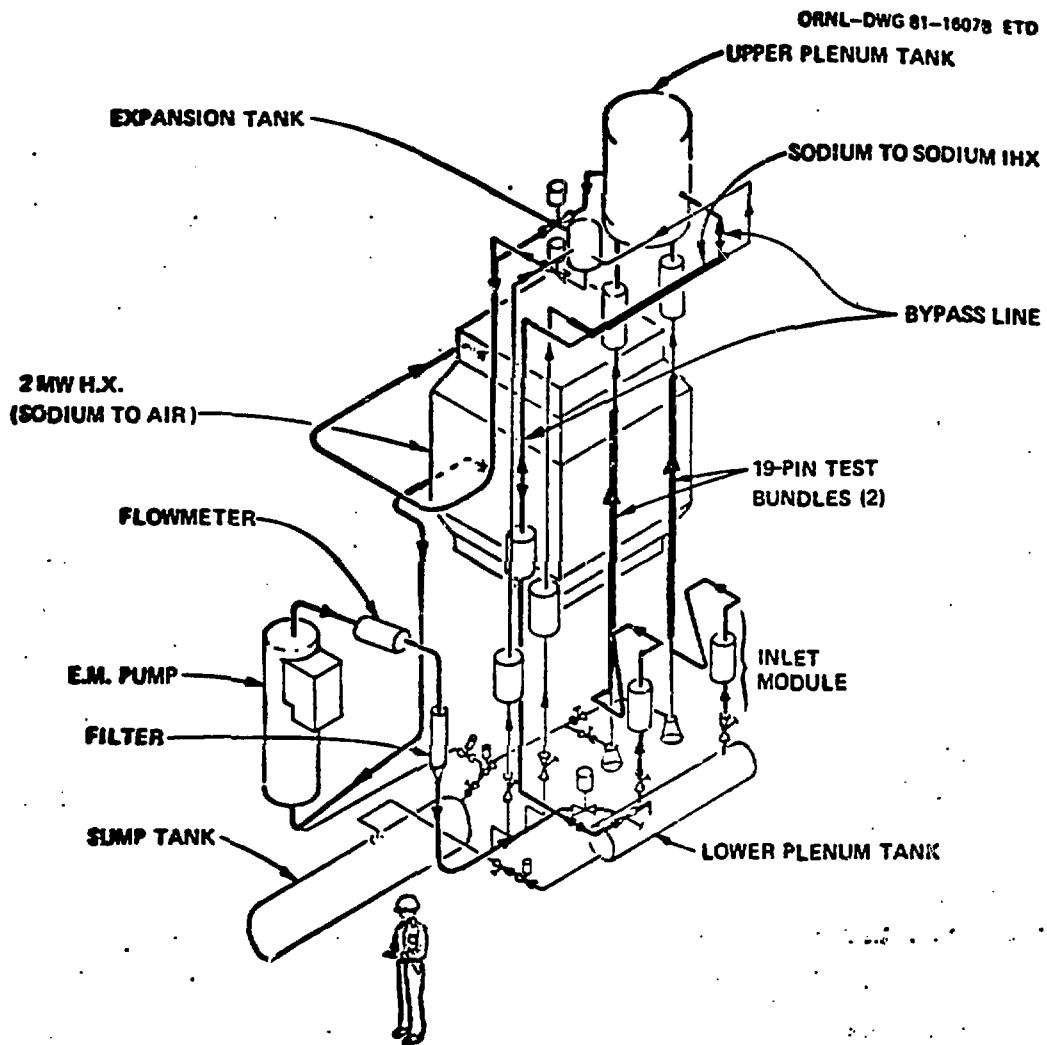


Fig. 1. THORS-SHRS facility isometric flow sheet.

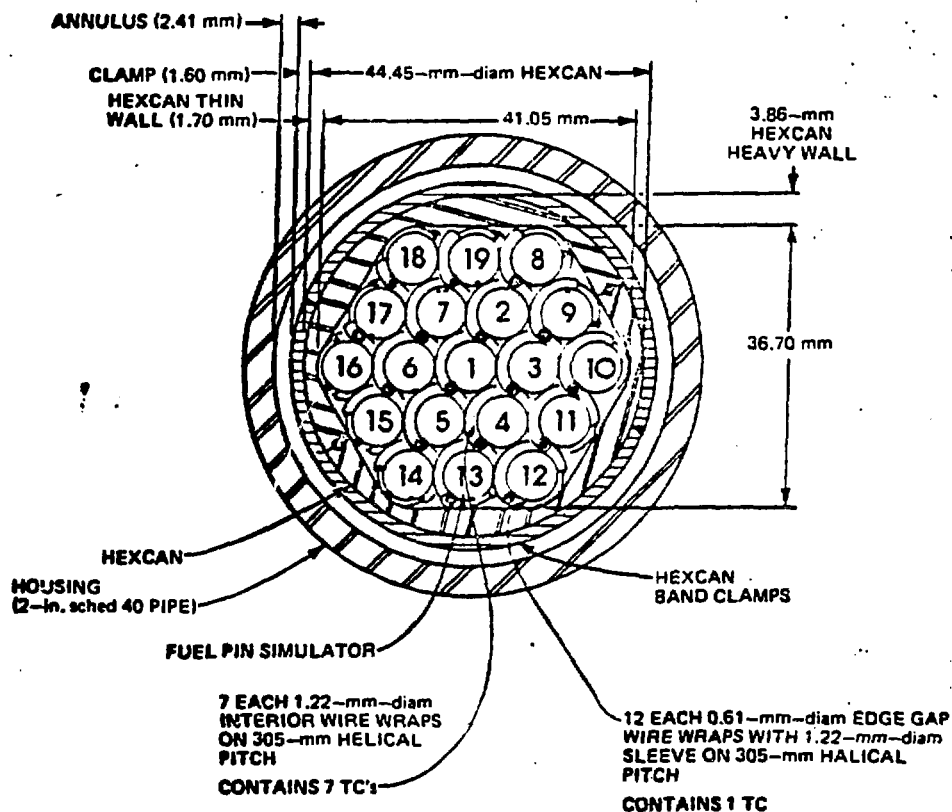
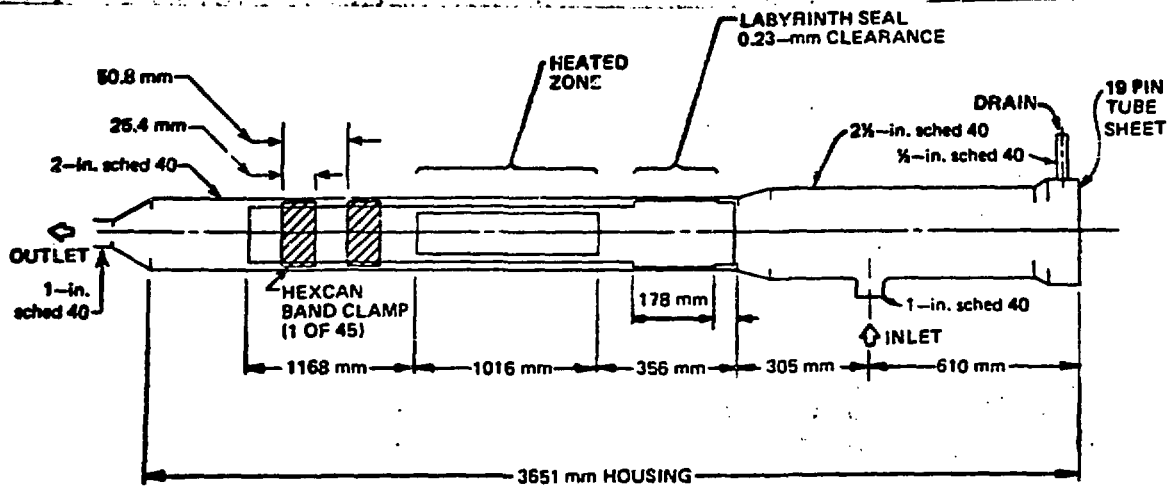


Fig. 2. Longitudinal and cross-sectional views of THORS-SHRS Assembly 1 bundle.

secondary flow. In the forced convection mode, the pump is used to supply flow to the bundles, and the bypass operates in upflow to provide a constant-pressure-drop boundary. The secondary side of the IHX is shut off and the component is not utilized as a heat exchanger. Heat rejection is accomplished by the 2 MW sodium-to-air heat exchanger. These flow paths are shown schematically in Fig. 3. All tests described in this paper were run in the forced convection mode.

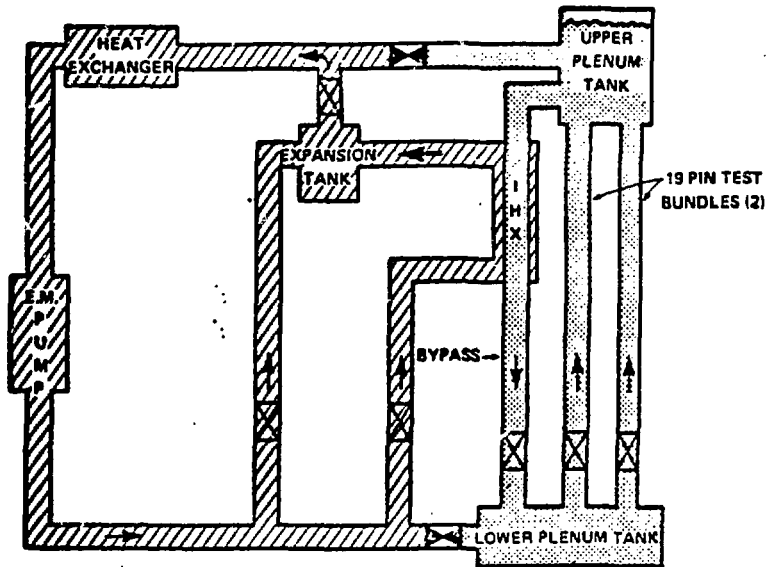
Description of the Test Bundles

The two bundles contain identical instrumentation. A detailed thermocouple layout is shown in Fig. 4. The FPSs are 6.99 mm in diameter, and have a heated length of 1016 mm. The axial heat flux profile is a chopped-cosine with a peak-to-average ratio of ~ 1.28 . The upper and lower axial blankets are simulated by 356 mm-long unheated zones immediately up- and downstream of the heated section; the simulated upper blanket contains sintered (porous) stainless steel pellets to provide a better simulation of the thermal behavior of this section in a reactor. Downstream of the upper blanket section is a hollow tube simulating the fission gas plenum. Each FPS contains three "heater-internal" thermocouples (TCs) as shown by the solid black dots in Fig. 4. These TCs rest on the inner wall of the FPS sheath.

The wire-wrap spacers are 1.22 mm in diameter, on a 305 mm helical pitch. Each of the wire-wraps on the seven internal pins contains seven TCs, indicated by the open circles around the FPSs in Fig. 4. The 12 outer wire-wraps contain only one TC each. This was necessary because the edge gap, between the duct wall and the outer FPSs, is half-size (0.61 mm) to reduce the flow-to-power ratio in these subchannels. The

oml

SHRS ASSEMBLY 1 IN NATURAL-CONVECTION MODE OF OPERATION



oml

SHRS ASSEMBLY 1 IN FORCED-FLOW MODE OF OPERATION

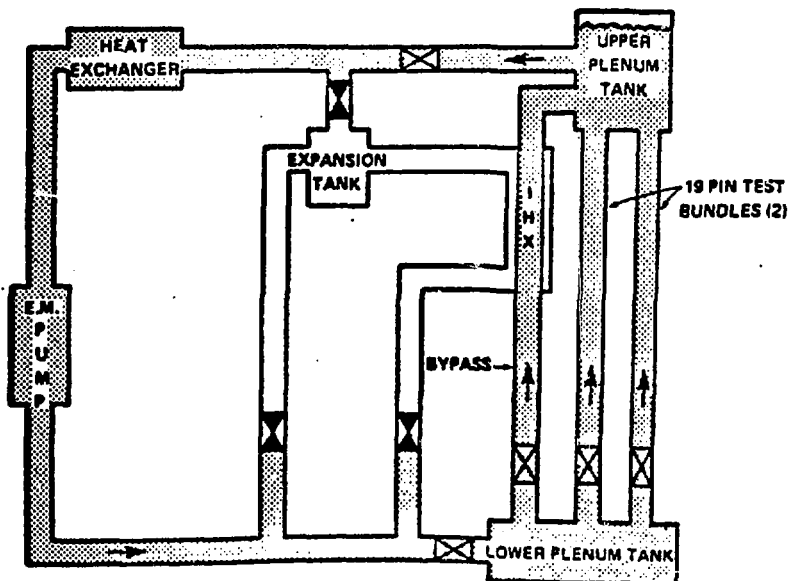


Fig. 3. Schematic diagram of THORS-SHRS Assembly 1, showing natural convection (top) and forced convection (bottom) flow paths.

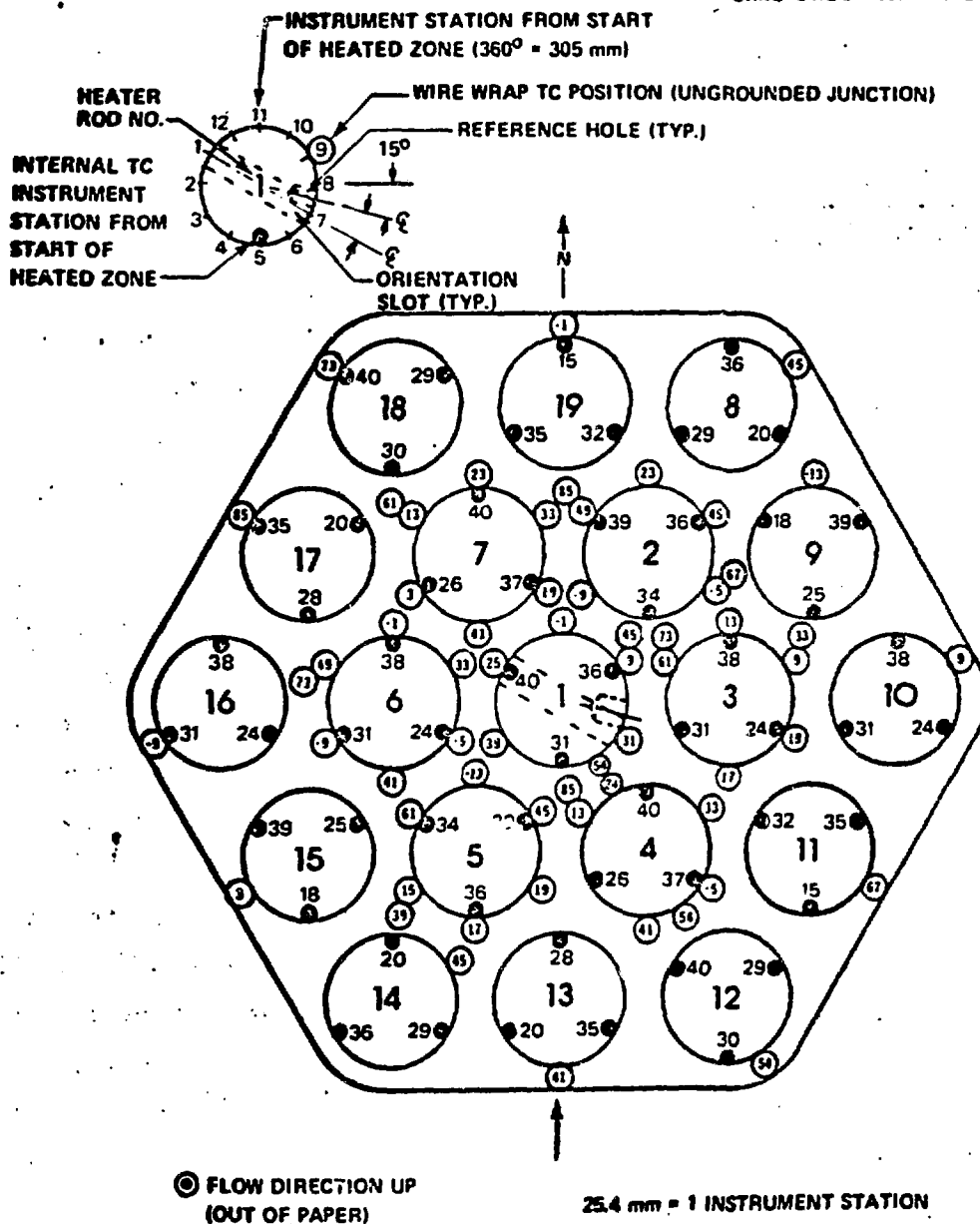


Fig. 4. THORS-SHRS Assembly 1 bundle thermocouple layout.

proper spacing in the interior subchannels is accomplished by sleeving the wire-wraps, but only one TC can be accommodated.

As shown in Fig. 4, several elevations of the bundles are instrumented with either heater-internal or wire-wrap TCs to allow bundle diametral temperature profiles to be observed. The axial stations at which this scheme was employed are: 31 (FPSs 16, 6, 1, 3, 10); 36 (FPSs 14, 5, 1, 2, 8); 40 (FPSs 18, 7, 1, 4, 12); and 45 (wire wraps on FPSs 14, 5, 1, 2, 8). These profiles were used for the comparison of steady state data from the two bundles.

Description of the Steady State Tests

The THORS-SHRS Assembly 1 test program consisted of four phases. The first of these was preliminary and shakedown testing, which included several single-phase, steady state tests to acquire baseline thermal-hydraulic data from the loop. One of these tests, Test 114, consisted of several steady state runs at various powers and flows, with the power-to-flow ratio never exceeding the nominal value (at 100% power and flow). These data were used in the inter-bundle comparison. A second test in this phase, Test 115, was used to help estimate the flow in the labyrinth seal between the outer wall of the bundle duct and the test section housing (see Fig. 2). This information was valuable in the analysis of the difference in the data from the two bundles.

Runs 107 and 1071 of test 114 were performed at 75% nominal power and 75% nominal flow, while Runs 110 and 1101 were performed at 10% nominal power and flow. These four runs were used to compare the behavior

of two bundles. In addition, since two runs at each power-flow combination were examined, it was possible to assess the reproducibility of the data from each bundle independently.

Results and Discussion of the Steady State Tests

Data from the four runs of Test 114 are presented in Figs. 5-8; each figure shows one diametral temperature profile. The TC temperature is normalized with respect to the inlet temperature and the overall bundle temperature rise, in order to eliminate the effect of small variations in bundle inlet temperatures and flows in the different runs.

Data from axial station 31 are shown in Fig. 5. The thermocouple on pin 6 in Bundle B did not operate properly in Runs 107 and 1071, and is not shown. In addition, for this figure and the three following, the position of the wire-wrap (WW) is indicated in pin 1, and the heater-internal thermocouples, where applicable, are shown in their nominal positions. The temperature "profiles" should not be taken as the actual bundle temperature structure; straight lines were used to connect these points for convenience.

Temperature data for axial station 36 are shown in Fig. 6, with the bundle rotated 60° clockwise for clearer presentation. The last profile derived from heater-internal TCs, at axial station 40, is presented in Fig. 7, with the bundle rotated 60° counterclockwise. The TC on pin 7 in Bundle A failed to operate in any of the tests, and is not shown. Finally, the profile derived from wire-wrap TCs at axial station 45 is shown in Fig. 8. Here, the TC on pin 2 failed in both bundles and is not shown at all.

TEST 114 – THORS–SHRS ASSEMBLY 1 HEATER–INTERNAL THERMOCOUPLE AT STATION 31

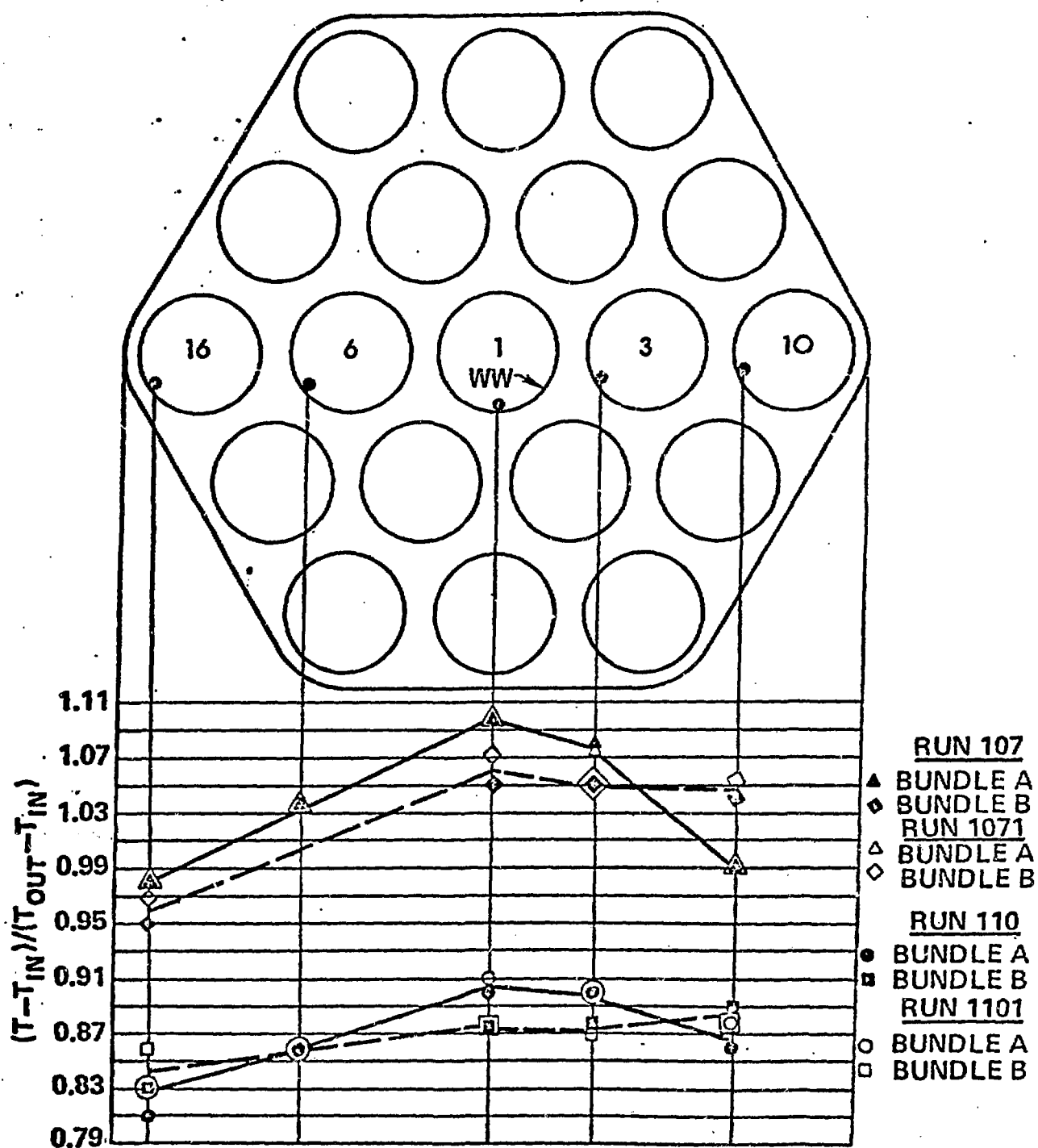


Fig. 5. Normalized heater-internal temperatures at station 31.

TEST 114 – THORS–SHRS ASSEMBLY 1 HEATER–INTERNAL THERMOCOUPLE AT STATION 36

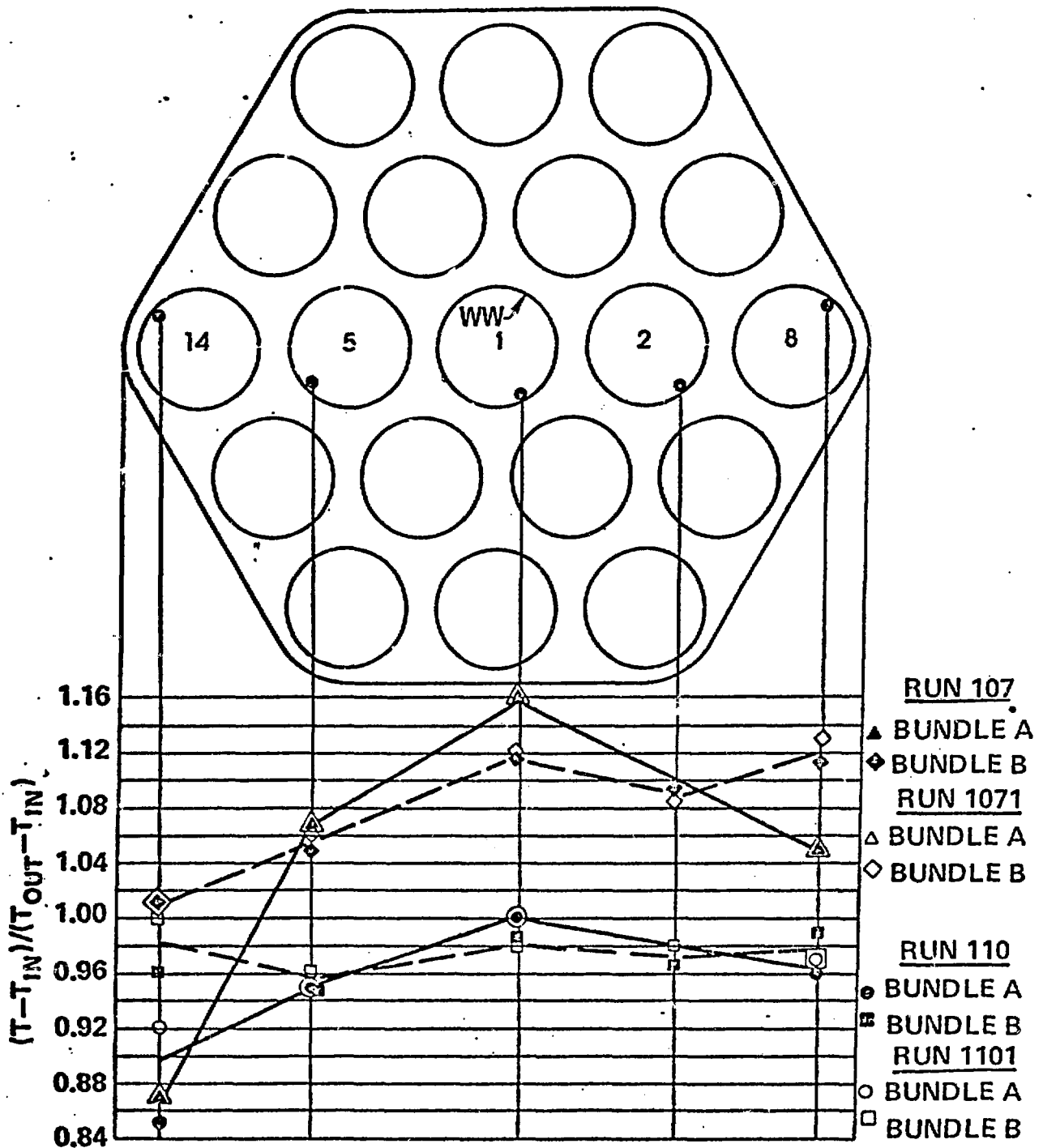


Fig. 6. Normalized heater-internal temperatures at station 36.

TEST 114 – THORS–SHRS ASSEMBLY 1 HEATER–INTERNAL THERMOCOUPLE AT STATION 40

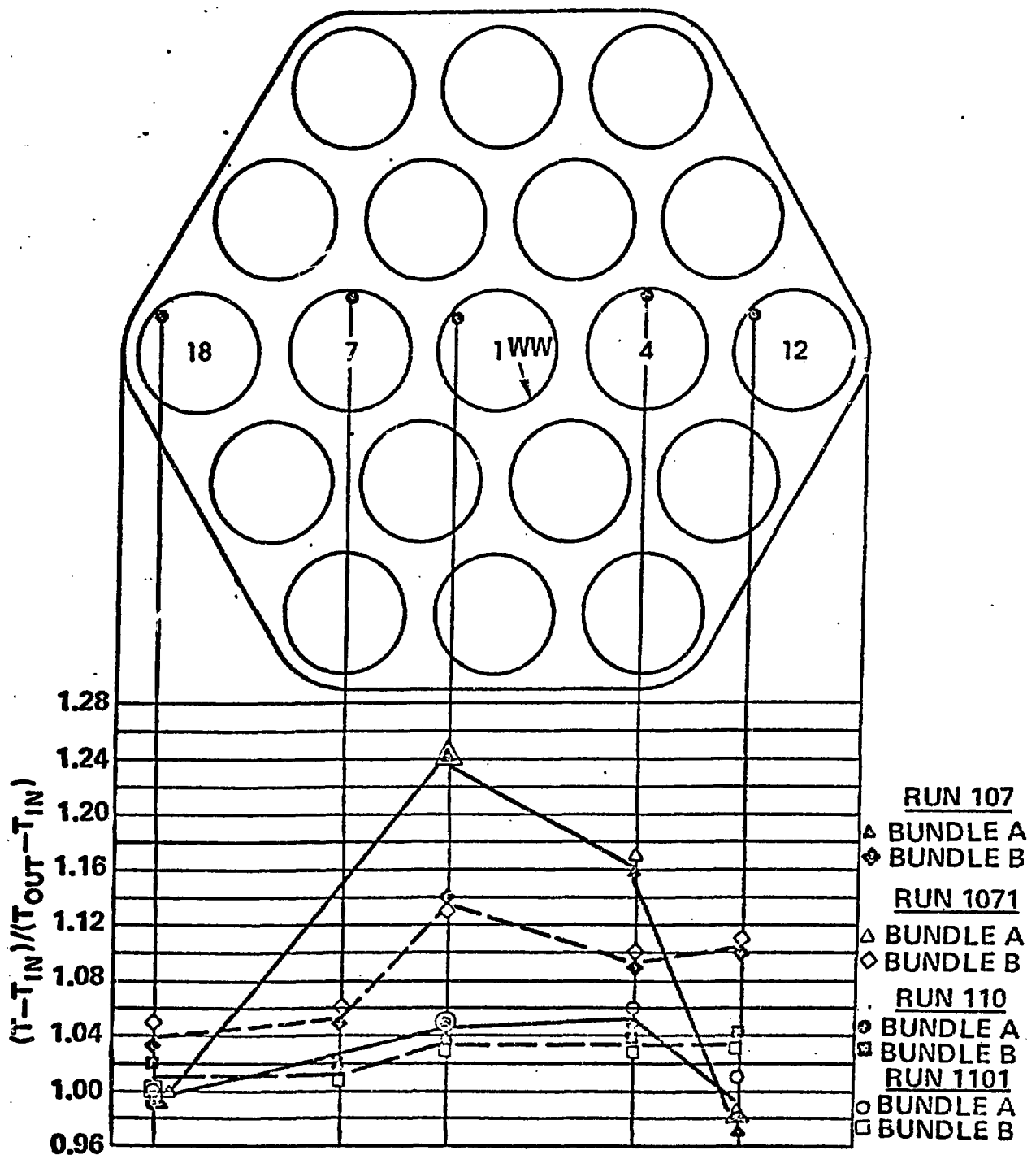


Fig. 7. Normalized heater-internal temperatures at station 40.

TEST 114 – THORS–SHRS ASSEMBLY 1

WIRE–WRAP THERMOCOUPLE

AT STATION 45

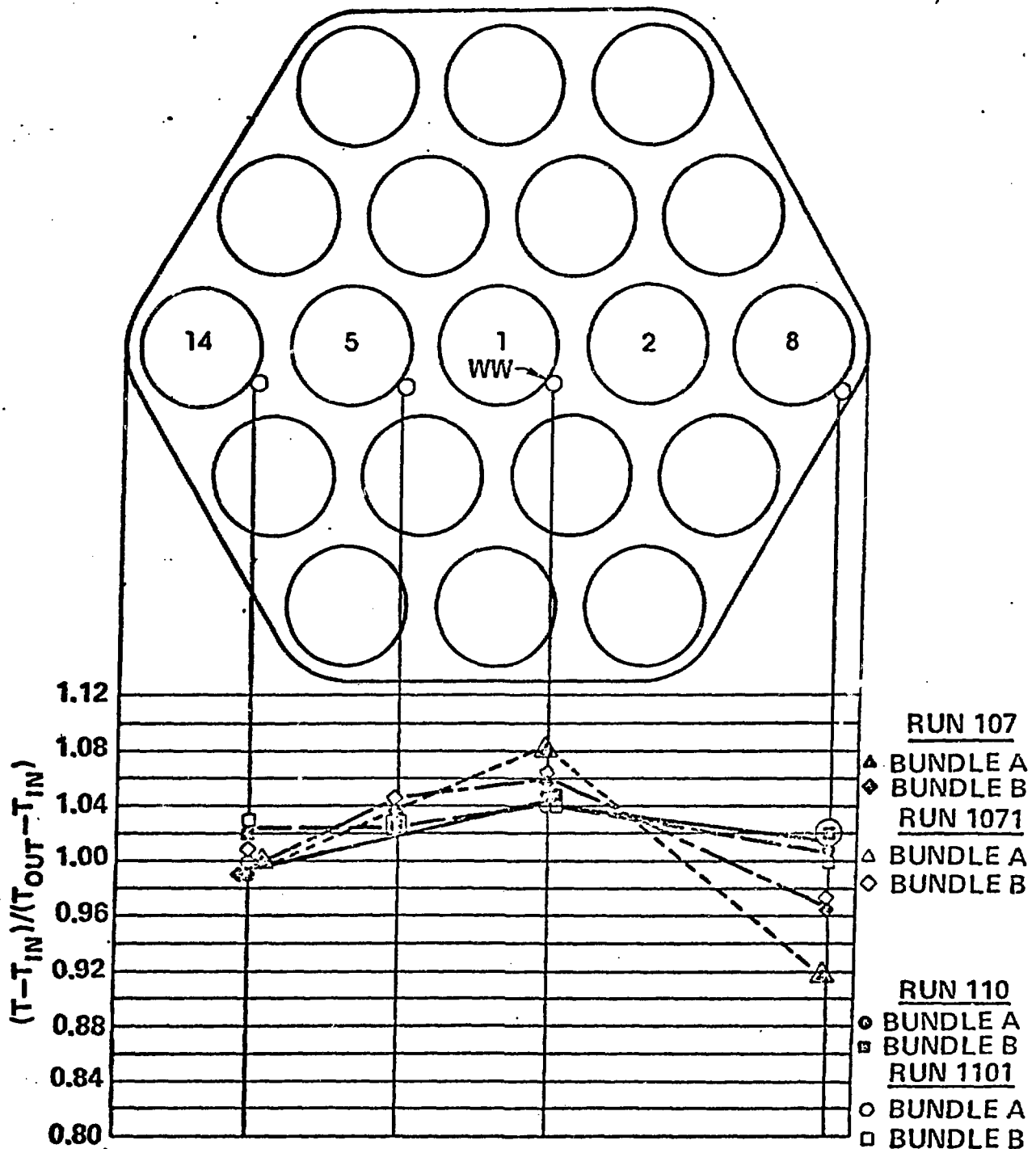


Fig. 8. Normalized wire-wrap temperatures at station 45.

Several facts are immediately apparent from the data. First, the high-power and -flow runs have much higher bundle-center temperatures, and more sharply peaked profiles, than the low-power and flow runs. This results from a combination of factors: the higher heat losses from the bundles and lower cladding temperature rises at lower powers tend to reduce overall bundle temperatures, while the mixed convective effects and radial conduction at lower flows tend to flatten bundle temperature profiles. Second, each bundle, in general, shows excellent data reproducibility in each set of two runs. Only the thermocouple at axial station 36 on pin 14 in Bundle A shows a substantial difference in Runs 110 and 1101. All other points agree extremely well. Reasons for differences and uncertainties in TC readings will be explored later in this section.

The third, and last, obvious point is that the data from the two bundles differ, in some cases, quite markedly. There are several possible explanations for this behavior.

The differences in the behavior of the two SHRS Assembly 1 bundles can be a result of several interacting factors, including construction, operation, bundle response to its environment, and intrinsic uncertainties. Although the bundles have identical design specifications, small variations in FPS, wire-wrap, and bundle duct dimensions occur because of manufacturing tolerances. Similarly, small variations in TC placement within FPSs and wire-wraps will occur, as well as small differences in overall heater-element resistance (contributing to power variations), and in the density of the boron nitride insulation used inside the FPS, which affect the center-to-sheath temperature drop. The differences in

TC placement become especially noticeable near the end of the heated section. For instance, in Fig. 7, the Bundle B temperatures are considerably below those in Bundle A, particularly in the high-power runs, on pins 1, 4, and 12. It is possible that the heater-internal TCs in Bundle A sit just inside the heated section, which ends at this axial station, while the Bundle B TCs are just outside of the heated zone. The presence of a center-to-sheath temperature drop in Bundle A versus the absence of such a drop in Bundle B at this elevation could explain the differences in the data.

The intrinsic uncertainties within each bundle also play a part in the inter-bundle variations, as well as differences between temperatures in two tests in the same bundle. During operation, the FPSs and wire-wraps can shift slightly from the effects of stress relief or thermal expansion and contraction. This slight radial movement of the TCs can have a considerable effect on the temperature of the TC, particularly in high-flow tests, where the temperature profile is sharply peaked. In addition, the intrinsic error for these TCs, according to their specifications, is $\sim \pm 1\%$ of reading. At the powers and flows in these tests, that error becomes ~ 0.033 in normalized temperature. The DAS also adds an associated error in converting the analog data to digital information. Combining these errors by root-sum-square means gives an estimate of $\sim \pm 0.034$ in normalized temperature.

A final contributor to differences between the behavior of the two bundles is the difference in thermal boundary conditions, as influenced by the flow through the labyrinth seal. A considerable amount of work was done to estimate the magnitude of this flow. As previously noted, a

small gap exists between the outside of the bundle duct and the test section housing (see Fig. 2). Although this gap, the labyrinth seal, has only a 0.23 mm annular clearance, its relatively large diameter makes its flow area ~9% of that of the bundle interior. To estimate the flow through this gap, Test 115 was included in the experimental program. The runs in this test consisted of a number of steady state power and flow combinations over the range of testing projected for the loop. The labyrinth seal flow was calculated using a heat balance on the bundle, calculated by two methods. First, a heat balance was calculated using the temperature difference between the test section outlet TC, which lies downstream of the point where the two streams converge, and the test section inlet TC. This heat balance, comparing heat transport in the bundle to the power input, would be unity if no heat were lost to environment. A second heat balance was then calculated using wire-wrap TCs in the simulated fission gas plenum, before the two streams converge. Three TCs were used, one in each ring of bundle sub-channels (see Fig. 4), to arrive at an area-weighted outlet temperature, called T^* . The entire test section flow was used for this calculation as well as for the first one. However, since the flow at the point of temperature measurement is less than the test section inlet flow, the heat balance percentage should be greater than the first one. Comparing these heat balances then gives an estimate for the labyrinth seal flow. While this measurement is only an approximation, due to uncertainties in power measurement, heat losses to the environment, and temperature and flow data, it does provide a reasonable estimate for the

labyrinth seal flow, and can serve to highlight differences in the behavior of the two bundles.

The results of these calculations are shown in Fig. 9. The calculation was performed twice for each bundle for each flow shown; where only one point appears, the two results were identical. As seen, the labyrinth seal flow in Test Section A begins at ~9% of the test section flow and decreases monotonically with flow. A considerable difference is seen in the behavior of Test Section B, however, where the labyrinth seal flow is ~5% at the highest flow, increases to ~6.5% as the flow decreases, and then decreases with test section flow until its behavior resembles that of Test Section A. A possible explanation for difference in behavior observed for the two test sections would be that Bundle B is inserted into its housing with a slight eccentricity. The shrinkage of the gap on one side of the bundle and widening thereof on the opposite side could account for this behavior, because of the change in pressure drop characteristics of an eccentric arrangement as a function of Reynolds number. This explanation would also account for the differences in bundle temperature structure, particularly near the edges of the bundle, observed in Test 114 for Bundle B. Referring to Figs. 5-8 once again, there is a marked difference in bundle-edge temperatures at every elevation on the right side of the bundle (pins 8, 10, 12). These temperatures are much higher than the corresponding temperatures in Bundle A, and the consistency of the results implies strongly that there is a systematic reason for the discrepancy, rather than random errors. The narrowing of the bundle-to-housing gap on this side, displacing high-conductivity liquid sodium, and the corresponding increase of the gap on

THORS-SHRS ASSEMBLY 1

LABYRINTH SEAL FLOW

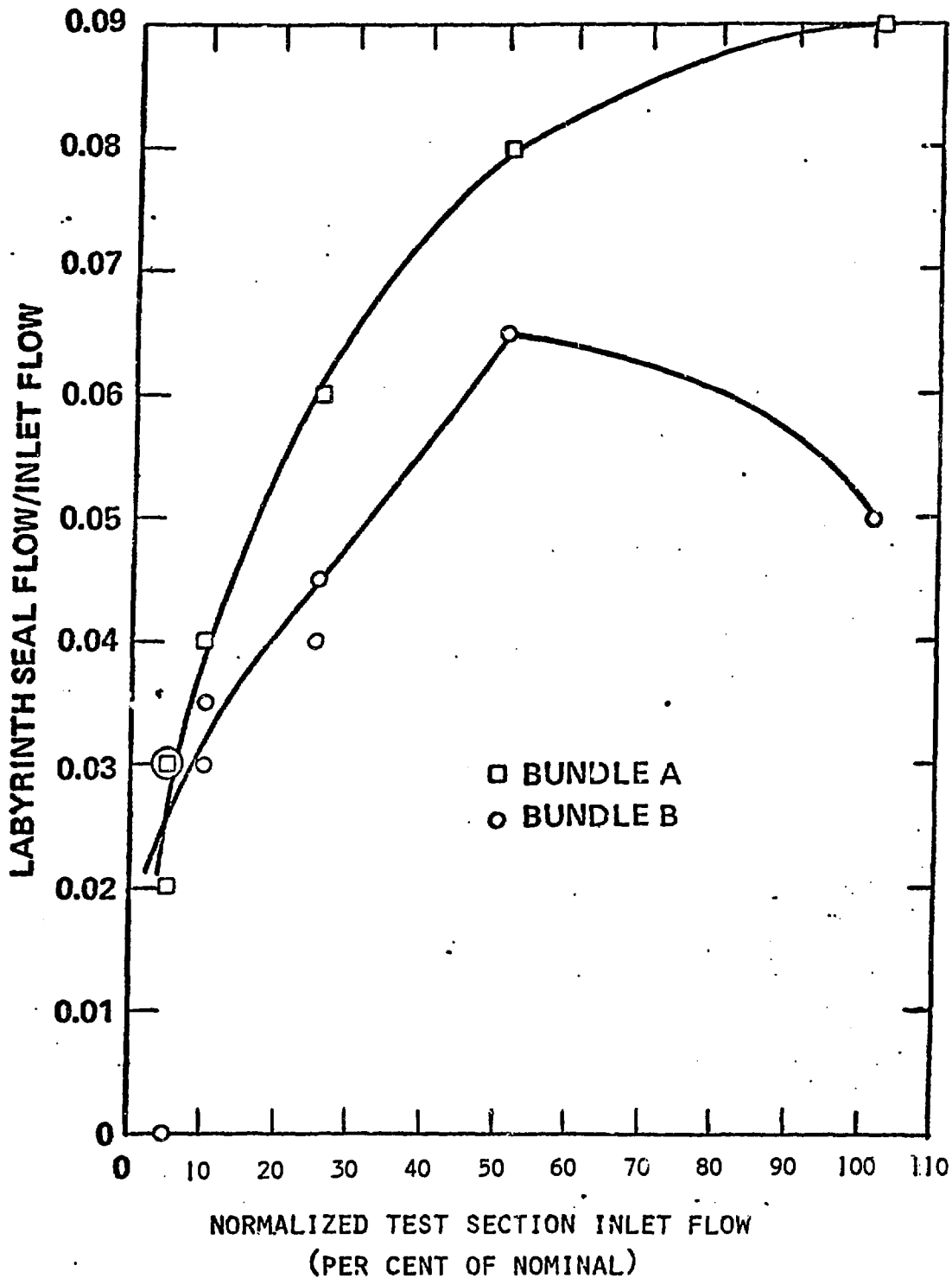


Fig. 9. Labyrinth seal flow as a function of test section inlet flow for Test Sections A and B.

the opposite side, would cause asymmetric heat transfer behavior and distort the bundle temperature profiles.

This discussion highlights the difficulty in comparing two bundles, even when they are nominally "identical." Clearly, small variations in the manufacture of components, and in the assembly and installation of these components, even where they are within strict tolerances, can have a substantial effect on the results obtained from these bundles. It is also clear that, in performing numerical analyses of THORS-SHRS Assembly 1, the differences in thermal boundary conditions must be taken into account. It would be expected that the behavior of the bundles at low flows would be similar, while at higher flows, greater differences would be observed, because of the similarities in labyrinth seal flows at low flows and their divergence at higher flows.

In addition to the specific application to the THORS facility, the results of this study also serve to emphasize the caution that all analysts must take in developing models and applying those models to thermal-hydraulic analyses, since the uncertainties and anomalies in experimental systems can have a great impact on the results of such work.

Conclusions

A comparison of temperature data from steady state tests in two parallel, simulated LMR bundles with identical design specifications has been performed. In general, the instrumentation functioned well, and results from the two bundles agreed quite well near the bundle center and at low flows. Differences were seen near the end of the heated zone of one bundle, which may be attributable to small differences in thermocouple locations. Variations were also seen near the bundle

edges, particularly at high flows. An analysis of the labyrinth seal flow around the outer surface of the bundle duct wall indicates that one of the bundles may be slightly eccentric in its alignment within the housing. This could change the thermal boundary conditions for that test section, and thereby cause the variations in temperatures observed near the bundle edges.

These results also serve to indicate the care that must be taken to account for uncertainties in analyzing thermal-hydraulic results.